

Smart sensors for monitoring crack growth under fatigue loading conditions

Victor Giurgiutiu[†], Buli Xu[‡], Yuh Chao^{††}, Shu Liu^{‡‡} and Rishi Gaddam^{‡‡‡}

Department of Mechanical Engineering, University of South Carolina, Columbia, SC 29208, USA

(Received January 5, 2005, Accepted November 11, 2005)

Abstract. Structural health monitoring results obtained with the electro-mechanical (E/M) impedance technique and Lamb wave transmission methods during fatigue crack propagation of an Arcan specimen instrumented with piezoelectric wafer active sensors (PWAS) are presented. The specimen was subjected in mixed-mode fatigue loading and a crack was propagated in stages. At each stage, an image of the crack and the location of the crack tip were recorded and the PWAS readings were taken. Hence, the crack-growth in the specimen could be correlated with the PWAS readings. The E/M impedance signature was recorded in the 100 - 500 kHz frequency range. The Lamb-wave transmission method used the pitch-catch approach with a 3-count sine tone burst of 474 kHz transmitted and received between various PWAS pairs. Fatigue loading was applied to initiate and propagate the crack damage of controlled magnitude. As damage progressed, the E/M impedance signatures and the waveforms received by receivers were recorded at predetermined intervals and compared. Data analysis indicated that both the E/M impedance signatures and the Lamb-wave transmission signatures are modified by the crack progression. Damage index values were observed to increase as the crack damage increases. These experiments demonstrated that the use of PWAS in conjunction with the E/M impedance and the Lamb-wave transmission is a potentially powerful tool for crack damage detection and monitoring in structural elements.

Keywords: Arcan specimen; crack growth; fatigue loading; piezoelectric wafer active sensor; electromechanical impedance; pitch-catch; Lamb wave.

1. Introduction

Structural health monitoring (SHM) is a major concern of the engineering community and SHM is especially important for detection and monitoring of crack growth under fatigue loading conditions.

Several health-monitoring methods exist, some **passive**, others **active**. The **active SHM** methods use smart sensors that can send and receive elastic waves in the structure. Thus, they can perform damage detection on demand. One type of smart sensor for active SHM is the piezoelectric wafer active sensor (PWAS), which is small, unobtrusive and can be permanently attached to a structure and left in place during operation (Lin and Yuan 2001 a,b,c, Giurgiutiu, Zagrai and Bao 2002, Ihn and Chang 2002). In

[†]Professor, Corresponding Author, E-mail: victorg@sc.edu

[‡]Ph.D. Candidate, E-mail: xub@enr.sc.edu

^{††}Professor, E-mail: chao@sc.edu

^{‡‡}Reserach Associate, E-mail: shu.liu@pw.utc.com

^{‡‡‡}Graduate student, E-mail: gar@enr.sc.edu

this work, two active SHM methods using PWAS transducers have been simultaneously considered (Giurgiutiu 2003). The two methods are: (a) the electromechanical impedance method and (b) the pitch-catch Lamb wave propagation. These methods were applied to an experiment performed on an Arcan specimen under fatigue loading. During the experiment, crack growth was monitored using digital imaging and active structural health monitoring. Nine PWAS transducers were mounted on the test sample and impedance signals from these transducers were taken at several crack lengths as the crack gradually propagated under fatigue loads. The crack tip locations were also marked on the specimen surface during the test so the actual crack lengths could be measured from the specimen surface after the test is completed.

1.1. Electro-mechanical impedance method

The electro-mechanical (E/M) impedance technique permits health monitoring, damage detection, and embedded NDE because it can measure directly the high-frequency local impedance which is very sensitive to local damage (Giurgiutiu 2002 and Park 2003). This method utilizes the changes that take place in the high-frequency drive-point structural impedance to identify incipient damage in the structure. Consider a PWAS transducer bonded to a structure. The structure presents to the PWAS transducer the drive-point mechanical impedance

$$Z_{str}(\omega) = i\omega m(\omega) + c(\omega) - ik(\omega) / \omega \quad (1)$$

Through the mechanical coupling between the PWAS transducer and the host structure, and through the electro-mechanical transduction inside the PWAS transducer, the drive-point structural impedance reflects into the electrical impedance as seen at the transducer terminals (Fig. 1).

The apparent electro-mechanical impedance of the PWAS transducer as coupled to the host structure is given by

$$Z(\omega) = \left[i\omega C \left(1 - \kappa_{31}^2 \frac{Z_{str}(\omega)}{Z_{PZT}(\omega) + Z_{str}(\omega)} \right) \right]^{-1} \quad (2)$$

In Eq. (2), $Z(\omega)$ is the equivalent electro-mechanical admittance as seen at the PWAS transducer terminals, C is the zero-load capacitance of the PWAS transducer, and κ_{31} is the electro-mechanical cross coupling coefficient of the PWAS transducer ($\kappa_{31} = d_{13} / \sqrt{\bar{s}_{11} \bar{\epsilon}_{33}}$). The PWAS is Z_{PWAS} . The E/M impedance method is applied by scanning a predetermined frequency range in the hundreds of kHz band and recording the complex impedance spectrum. The frequency range must be high enough for the signal wavelength to be compatible with the defect size.

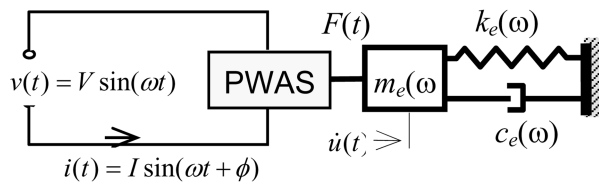


Fig. 1 Electro-mechanical coupling between the PWAS transducer and the structure

1.2. The Lamb wave propagation

The PWAS were also used as transmitters and receivers of Lamb waves in the specimen. When such waves encounter a defect, such as a crack, the waves get scattered. From the comparison of the pristine and damaged wave signals, the scatter signal can be extracted. Analysis of the scattered signal permits the correlation of the wave propagation recording with the damage progression (Lin and Yuan 2001a, Liu, *et al.* 2003, Giurgiutiu 2003, Ihn 2003).

2. Experimental setup and procedure

2.1. The Arcan specimen and test fixture

The Arcan specimen (Fig. 2) was made out a 1.2 mm thick galvanized mild steel sheet with yield

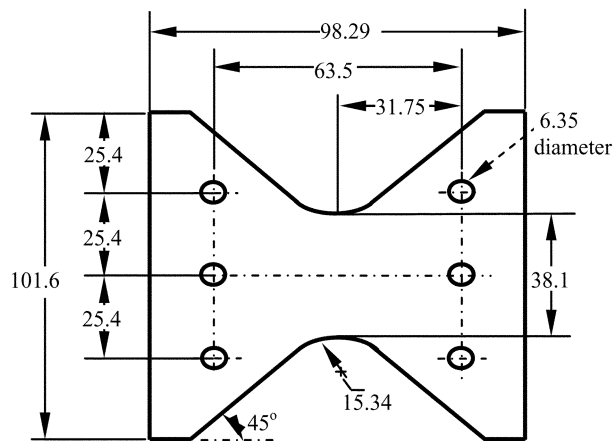


Fig. 2 Arcan specimen geometry (dimensions in mm)

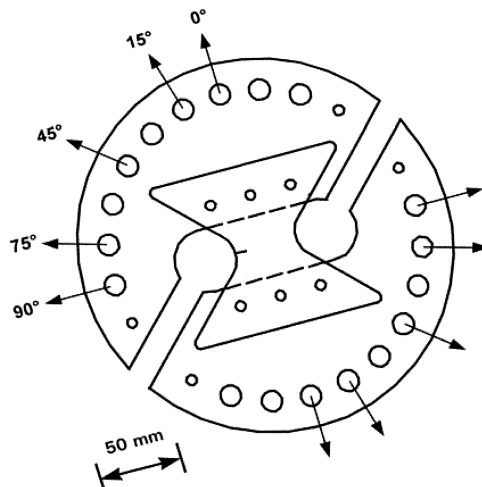


Fig. 3 Arcan specimen held inside the fixture

stress of 231 MPa and ultimate tensile stress (UTS) of 344 MPa. The fracture toughness (K_{Ic}) of the material is $140 \text{ MPa}\cdot\text{m}^{0.5}$. The Arcan specimen was designed for mixed mode I/II fracture testing with the fixture (Fig. 3). As shown in Fig. 3, a tensile load applied in the 0 (90) degree direction yields pure mode I (II) loading in the specimen. Loading in any of the intermediate angles, i.e., 145, 45, 75 degrees, generates mixed-mode loading (I/II) with a particular mode mixity.

2.2. Generation of controlled damage

Generation of controlled damage in experimental specimens is a major concern for any health monitoring and damage detection experiment. In the present study, our primary goal was to correlate changing E/M impedance signals and in pitch-catch transmission of elastic waves with varying levels of fatigue damage in the Arcan specimen. Hence, a repeatable method of identifying and quantifying specimen damage at any point in time was devised. This method consisted of pre-cracking the specimen in Mode I fatigue, and then propagating an inclined crack in Mixed Mode Fatigue. The propagation was done in stages, such that the crack damage at each stage could be measured and quantified.

2.3. Loading conditions

Fatigue load was applied using an MTS 810 Material Test System (Fig. 4), with 1 Hz to 10 Hz loading rate.

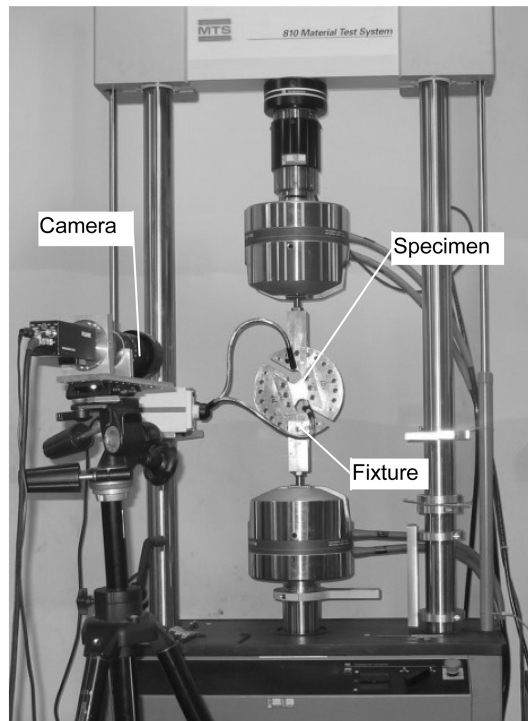


Fig. 4 Arcan specimen mounted in the MTS 810 Material Test System for fatigue crack propagation studies

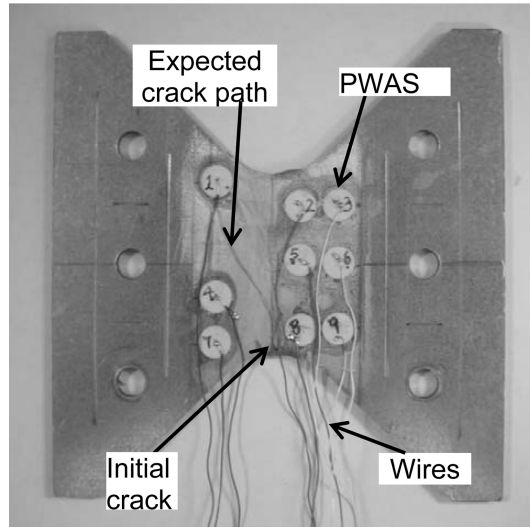


Fig. 5 Arcan specimen instrumented with nine PWAS transducers

2.3.1. Fatigue pre-cracking

First, the Arcan specimen was pre-cracked in Mode I fatigue loading to a 7.6 mm long edge crack which makes the initial $a/w = 0.2$, where a is the initial crack length and w is the width of the specimen ($w = 38.1$ mm). The maximum stress intensity factor (K_I) value in the first stage for fatigue pre-cracking was $16.07 \text{ MPa}\cdot\text{m}^{0.5}$ and the maximum stress intensity factor (K_I) value for the last stage for fatigue pre-cracking was $22.7 \text{ MPa}\cdot\text{m}^{0.5}$.

2.3.2. Mixed-mode fatigue cracking

Then, the specimen was subjected to mixed-mode fatigue loading by applying a load along the 75° direction of the holding fixture (Fig. 3). This gave a mode mixity $\beta = \tan^{-1}(K_I / K_{II}) = \tan^{-1}(13.354 /$

Table 1 Crack growth history and relative crack size ($R = 0.1$)

Stage	Max. Load (N)	Fatigue cycles	ΔK_I ($\text{MPa}\cdot\sqrt{\text{m}}$)	ΔK_{II} ($\text{MPa}\cdot\sqrt{\text{m}}$)	Crack growth (mm)	Crack size (mm)	Relative crack size
1	11121	39,500	11.878	29.339	Ref.	0.00000	0%
2	10231	49,500	37.657	3.472	0.50229	0.50229	3%
3	11121	51,500	43.349	3.080	0.44648	0.94877	5%
4	10231	56,700	42.437	2.339	0.39067	1.33944	8%
5	9341	62,723	46.811	3.082	2.00917	3.34861	19%
6	8452	71,100	50.294	3.733	2.34404	5.69265	33%
7	7562	77,547	49.624	4.343	1.50688	7.19953	42%
8	6672	79,000	47.009	0.176	1.00458	8.20411	47%
9	6672	80,775	52.503	0.074	1.78593	9.99004	58%
10	5783	86,870	51.602	-0.952	2.00917	11.99921	69%
11	5783	91,800	56.041	-4.385	1.39526	13.39447	77%
12	5783	94,000	69.832	-14.450	3.90673	17.30120	100%

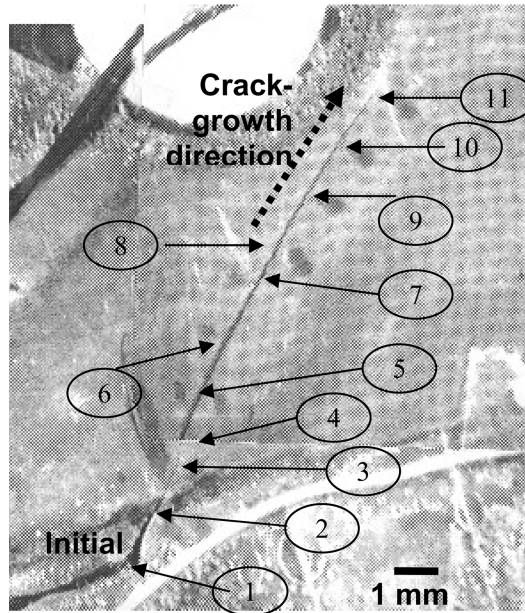


Fig. 6 Close-up image showing the crack-tip location after each stage up to stage 11. The arrow marked “1” shows the location of the tip of the fatigue pre-crack

41.163) = 0.314 which is a Mode II dominant loading. The initial maximum load was 11.12 kN (2500 lb). The loading was done in stages, such that the specimen did not fail instantaneously after the crack has grown by a certain length. The loading ratio (Max_Load/Min_Load) was $R = 0.1$. The load values are given in Table 1. A frequency between 1 Hz and 10 Hz was used in each stage for the fatigue loading to control the crack-growth rate as the crack-length increased. The crack hence grew in stages with a different loading rate for each stage. The overall crack path is shown in Fig. 6.

2.4. Specimen instrumentation and measurements

2.4.1. Specimen Instrumentation

The specimen was instrumented with nine circular PWAS as shown in Fig. 5. The PWAS were made from APC-850 piezoceramic wafers of 7 mm diameter and 0.200 mm thickness from APC International, Inc. The PWAS were mounted on one side the specimen. Care was given to keeping the PWAS away from the expected crack path (Fig. 5). The transducers were wired and numbered. Through the process, the electrical integrity of the transducers was measured for consistency.

In addition, a digital camera was used to take close-up digital image measurements of the specimen at various stages of the testing program.

2.4.2. Measurements

A digital image of the specimen was taken after each fatigue loading stage, using image capture software. In addition, a reference mark was made near the crack tip to mark the crack progression after each loading stage.

The PWAS data was also recorded after every stage so that the crack-growth data from the images

and the data from the PWAS could be compared. The PWAS data was taken with two methods (i) the E/M impedance method; and (ii) the Lamb wave propagation method. For the impedance method, a Hewlett Packard 4194A Impedance Analyzer was used. The E/M impedance signatures of the 9 PWAS transducers affixed to the specimen was taken and stored in the PC. In initial trials, the frequency range 100 kHz to 500 kHz was determined as best suited for this particular specimen.

For the Lamb-wave propagation method, the pitch catch approach was used. A three-count tone burst sine wave at a frequency of $3 \times 158 \text{ kHz} = 474 \text{ kHz}$ and 10 Vpp amplitude was generated with a HP33120 function generator. In a round-robin fashion, the excitation signal was applied to one of the PWAS working as a transmitter. The signals received at the other PWAS were recorded with a Tektronix TDS210 digital oscilloscope.

3. Results

The test proceeded in twelve crack-growth stages. The overall crack-growth fracture path recorded during the test is shown in Fig. 6 with arrows pointing to the tip location corresponding to each growth stage. Finite element analyses were performed using FRANC2D/L (2000) for each stage of the crack growth to determine the stress intensity factors KI and KII applied to the crack tip. The calculated K_I and K_{II} values are also included in Table 1. Fig. 6 shows that the crack grew kinked relative to the initial crack direction (stages 1 to 2) which is in agreement with the direction of tensile fracture (Chao and Liu 1997, 2004). After the initial cracking, the crack growth followed the path for tensile fracture (stages 2 through 12) until instability occurred (stage 12, not shown in Fig. 6). This fact is reflected by the K_I and K_{II} values as well, i.e., the initial crack (stage 1) is Mode II dominant and it becomes Mode I dominant immediately after the crack growth (stages 2 and thereafter).

3.1. Damage quantification

Damage quantification and control was performed using the crack length. The maximum crack length ($a_{\max} = 17.3 \text{ mm}$) was taken to correspond to maximum damage and was assigned a value of 100% damage. The other intermediate damage cases were assigned damage values proportional with the relative crack size (i.e. % damage = a/a_{\max}). Thus, we could monitor and control the amount of damage accumulating in the fatigue specimen (Table 1).

3.2. Health monitoring under controlled damage conditions

The relative crack length was used to identify the damage amplitude and control the damage progression in the Arcan specimen during the fatigue testing. Our purpose was to stop the loading and collect health-monitoring data at various damage values. This was achieved by stopping the experiment when the relative crack length was 3%, 5%, 8%, 19%, 33%, 42%, 47%, 58%, 69%, 77% and 100%. All the measurements were taken in the same room temperature to exclude temperature influence on the measurement readings.

At each damage value, the readings of the E/M impedance signature of the nine PWAS transducers stored in the PC were analyzed. Also analyzed were the readings taken of the pitch-catch transmission of Lamb waves between various PWAS (#3 to #1; #3 to #4; #3 to #7; #6 to #1; #6 to #4; and #6 to #7). The process was repeated for each crack length up to the maximum value (17.3 mm at

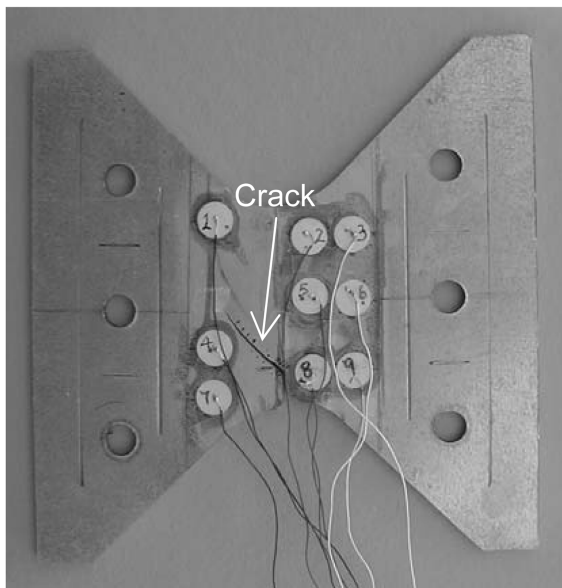


Fig. 7 Cracked Arcan specimen with final crack size 17.3 mm

94,000 cycles). Fig. 7 presents the cracked Arcan specimen with the crack at its maximum position (17.3 mm). Examination of the crack path reveals the intermediate crack tip positions marked with red dots.

During the fatigue loading, a number of PWAS showed insufficient adhesion durability and became disbonded from the specimen. This can be attributed to the plasticity effect near the crack-tip and to other fatigue-related aspects. This disbond may be due to the adhesive specification, and will be investigated separately. For the purpose of this paper, we note that PWAS #2, 5, 8 disbonded early in the experiment and will be discarded. Other PWAS disbonded only late; in this case, their readings will be retained up to the point when they became disbonded. For example, PWAS #1 disbonded just before the last two readings. Hence, only the last two readings of PWAS #1 are discarded.

4. Discussion

4.1. Damage effect on PWAS readings

In this specimen, the damage appeared in the form of a progressive crack, initiated at the specimen boundary and propagating diagonally across the specimen under mixed mode fatigue loading. As the crack advances, the effective high-frequency mechanical impedance seen by the PWAS attached to the specimen changes. This reflects in changes in the E/M impedance spectrum (Fig. 8a).

The crack propagation also induces changes in the path of Lamb transmission across the specimen. This modifies the signal waveform arriving at the receiver PWAS (Fig. 9). These two effects, E/M impedance change and Lamb wave transmission change, are different in nature, but complementary. The E/M impedance change is a high-frequency standing waves effect, while the Lamb-wave transmission change is due to waves being reflected and diffracted by the crack.

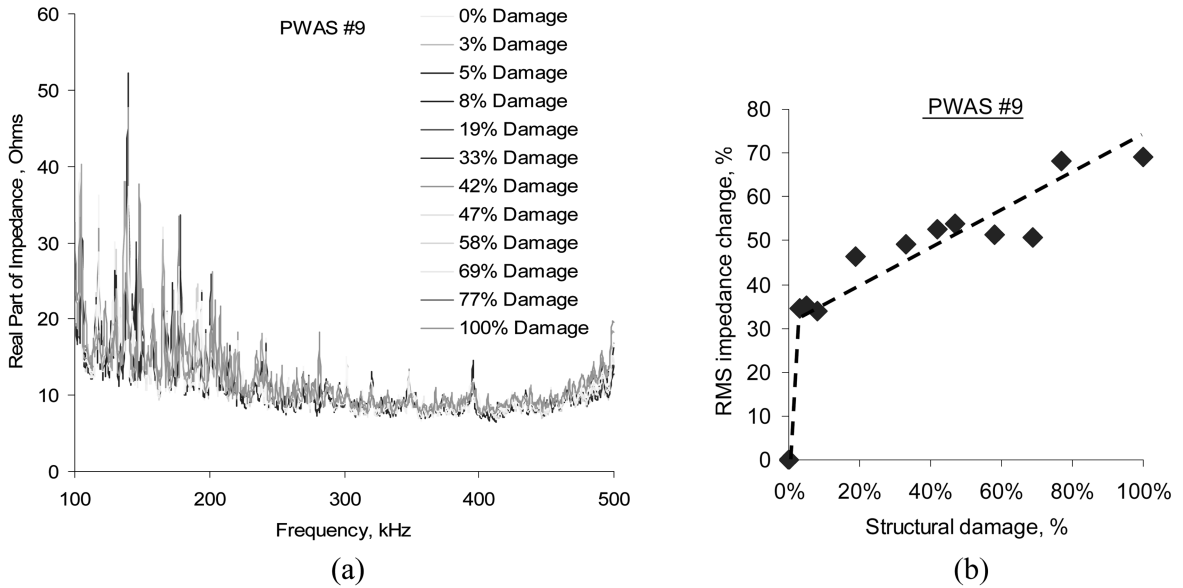


Fig. 8 PWAS #9 E/M impedance plots: (a) superposed E/M impedance plots; (b) RMSD damage index from E/M impedance

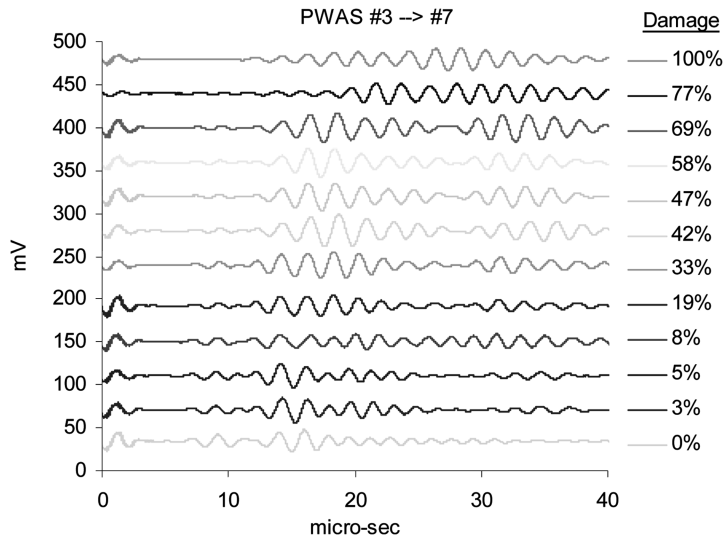


Fig. 9 Pitch-catch plot from PWAS #3 to PWAS #7

4.2. Correlation of E/M impedance readings with crack progression

Fig. 8(a) presents typical superposed plots of the impedance signatures obtained at various levels of damage. The impedance signature considered here is the real part of the complex E/M impedance, real Z , measured in the 100-500 kHz frequency band selected during pre-trial tests. Examination of the graphs in Fig. 8(a) reveals important modifications taking place in the impedance signatures due to the intricate

structural response changes induced by damage progression. However, direct interpretation of these impedance signatures is not straightforward.

A more direct interpretation is attained with a *damage index*. The damage index is a scalar quantity that is evaluated from the comparison of impedance signature at a given damage level with a baseline signature. In our experiment, we took as baseline the signature at the start of the tests. The mathematical expression of the damage index depends on the choice of damage metric. In this work, we used a damage index based on the Euclidean norm, i.e., the RMS impedance change calculated as:

$$\text{RMS Impedance Change, \%} = \left(\frac{\sum_N (\text{Re}Z_i - \text{Re}Z_i^0)}{\sum_N [\text{Re}(Z_i^0)]^2} \right)^{1/2} \quad (3)$$

where N is the number of sample points in the impedance signature spectrum, while the superscript 0 signifies the initial (baseline) state of the structure.

Examination of the E/M impedance data reveals changes recorded in the E/M impedance signatures with the progression of damage. These changes are reflected in both the E/M impedance signatures (Fig. 8a) and in the RMS impedance change damage index (Fig. 8b). Examination of Fig. 8(a) indicates that significant changes took place in the E/M impedance signature as damage progressed through the specimen. New frequency peaks appeared while other peaks were shifted or accentuated. Examination of the damage index plot (Fig. 8b) shows that the RMS impedance change increases monotonically with structural damage.

4.3. Correlation of Lamb-wave transmission readings with crack progression

Examination of the pitch-catch signals presented in Fig. 9 indicates that the crack size strongly influences the transmission of Lamb waves in the specimen. At the beginning (0% damage) the transmission of Lamb waves from PWAS #3 to PWAS #7 is direct and unimpeded, resulting in a representative arrival signal in the 10 to 20 micro-sec region (see the 0% curve in Fig. 9). As the crack extends, it progressively interferes with the direct wave path and the signal starts to change (see the 3% and 5% curves in Fig. 9). These changes become stronger and stronger as the crack extends (see the 8% through 69% curves in Fig. 9). Eventually, the crack has extended so much that it obliterates completely the direct wave path and no signal arrives any longer in the 10 to 20 micro-sec region (see the 77% and 100% curves in Fig. 9). In this latter case, the waves arrive on a round about path, i.e., in the 20 to 30 micro-sec region. Also apparent in the signal is the effect of wave dispersion and scatter.

The aforementioned damage index technique is again applied to find the direct relationship between the change of transmission of lamb waves and the crack growth. Since pitch-catch signals are getting weaker and weaker due to the increasing of crack size, two damage metrics including RMSD and power deviation are employed to calculate damage index. The mathematical expression for root mean square deviation (RMSD) was given in Eq. (4).

$$\text{RMSD} = \sqrt{\frac{\sum_{j=1}^n (y_j - x_j)^2}{\sum_{j=1}^n x_j^2}} \quad (4)$$

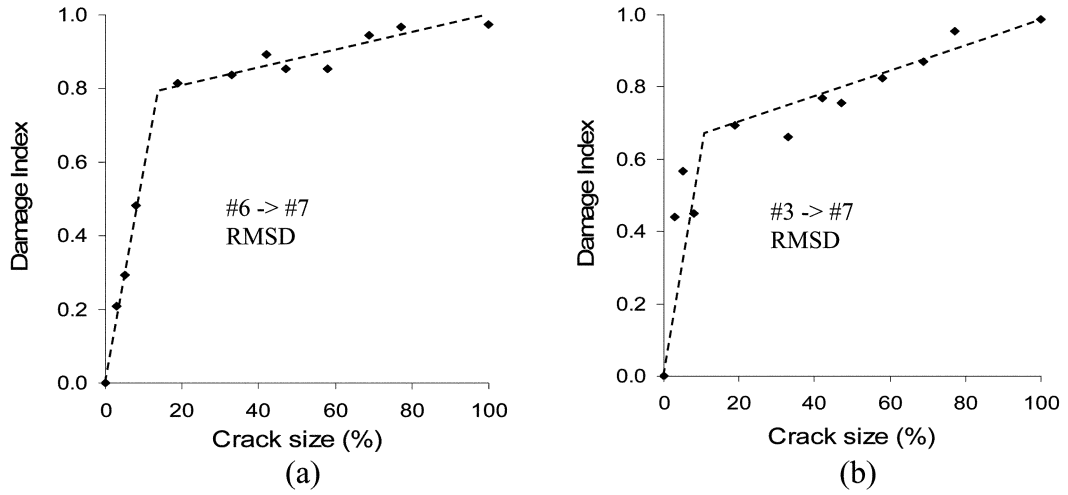


Fig. 10 Plot of RMSD (root mean square deviation) damage index from Pitch-catch method: (a) PWAS #6 to PWAS #7; (b) PWAS #3 to PWAS #7

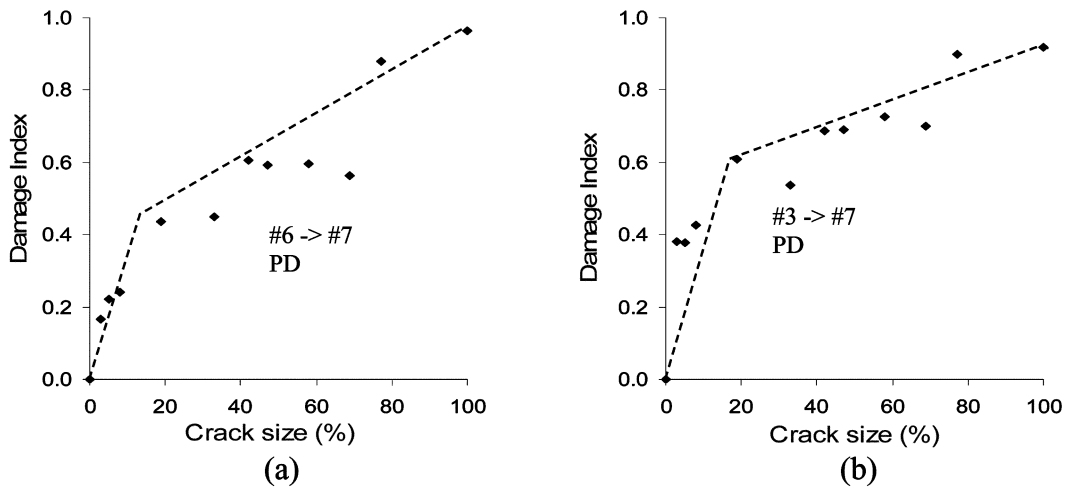


Fig. 11 Plot of PD (power deviation) damage index from Pitch-catch method: (a) PWAS #6 to PWAS #7; (b) PWAS #3 to PWAS #7

To monitor the power change in pitch-catch signals with the growth of crack, power deviation (PD) defined in Eq. (5) was also used.

$$PowerDeviation = 1 - \sqrt{\frac{\sum_{j=1}^n y_j^2}{\sum_{j=1}^n x_j^2}} \quad (5)$$

Where, n is the number of sample points, x signifies the pristine (baseline) pitch-catch waveform, and y signifies current pitch-catch waveform.

Note that when using RMSD and PD metrics to calculate damage index, it is very important to eliminate DC value in pitch-catch signals and make sure signals are synchronized in time. Fig. 10 to Fig. 11 show the damage index over crack size from pitch-catch signals by using RMSD and PD damage metrics. We can see that RMSD metric works better than PD metric for monitoring Arcan specimen crack growth under loading. When the crack is small, the reflection of waveforms from the transmitter is increasing with the growth of crack. A linear relationship between damage index and crack size can be perceived. With further growth of crack, the received waveforms are mainly scattered waves.

The rate of change of scattered waves according to crack growth is not as strong as before.

5. Conclusions

The application PWAS smart sensors to the active health monitoring of crack growth in an Arcan specimen under fatigue loading has been presented. In the past, PWAS transducers have been used for health monitoring of structures but they have not been used to record the crack-growth data under mixed mode crack growth in an Arcan specimen test. To the authors' knowledge, this is the first that such an experiment has been conducted.

5.1. Summary of main results

The work presented in this paper indicates that the E/M impedance method and the Lamb-wave propagation method applied with PWAS transducers are both able to detect the presence and advance of a crack under fatigue loading. The preliminary analysis of the data indicates that both the E/M impedance and the Lamb-wave propagation method can detect the presence and progression of a crack in an Arcan specimen. Further signal analysis and interpretation work is needed to reach the full potential of this experimental study.

During the fatigue loading, a number of PWAS transducers became debonded. This happened in the high-strain regions near the crack tip. This aspect must receive special attention in order to determine the strain limits of the current PWAS adhesion methods and to develop methods for a better and more durable adhesion of the PWAS transducers. In addition, sensors along the crack growth line were damaged. Sensors that survived off the crack line were used to monitor crack growth. For Arcan specimen, the crack growth line could be theoretically predicted; this enabled us to avoid mounting sensors along the crack-growth line and to use fewer sensors.

The measurements were taken at controlled temperature in order to avoid temperature effects on impedance spectrum. In practical implementations, multiple baselines under known environmental conditions in order to construct a comprehensive baseline database. When monitoring the structure, environmental conditions will be also monitored such that appropriate baselines are used in the comparison process.

5.2. Advantages of the present approach

The present paper has presented a combined approach in which optical and piezoelectric methods for crack detection and monitoring were combined. The optical equipment can be used to spot the crack-tip and it would be the surface defect that the equipment used could show to us; more sophisticated and higher magnification equipment might show even better the exact location of the crack tip. Even if the

crack tip is not visible on the surface, there might be defect induced under the surface of the specimen. Optical equipment cannot detect under the surface cracks. PWAS transducers were used to record the E/M impedance and the Lamb wave propagation data on the Arcan specimen. Hence, if there is any defect (crack) in the material, the data obtained from the PWAS transducers would be modified by the presence of the crack. The correlation of the PWAS data with crack-growth optical data in a specimen would yield an improved methodology for crack detection and monitoring in critical structures.

Acknowledgements

The financial support of National Science Foundation award # CMS 0408578, Dr. Shih Chi Liu, program director, and Air Force Office of Scientific Research grant # FA9550-04-0085, Capt. Clark Allred, PhD, program manager are gratefully acknowledged.

References

- Chao, Y. J. and Liu, S. (1997), "On the failure of cracks under mixed-mode loads", *Int. J. Fract.*, **87**(3), 201-223.
- Chao, Y., Liu, S. and Gaddam, R. (2004), "Fracture type transition under mixed mode I/II quasistatic and fatigue loading conditions", *Proceedings of the Annual Meeting of Experimental Mechanics*
- Chang, F.-K. (1995), "Built-in damage diagnostics for composite structures", *Proceedings of the 10th International Conference on Composite Structures (ICCM-10)*, Vol. 5, Whistler, B. C., Canada, August 14-18, 1995, 283-289.
- FRANC2D/L (2000), "A crack propagation simulator for plane layered structures, version 1.4 User's guide", D. Swenson and M. James, Kansas State University · Manhattan, Kansas, 2000.
- Giurgiutiu, V., Zagari, A. N. and Bao, J. (2002), "Piezoelectric wafer embedded active sensors for aging aircraft structural health monitoring", *Structural Health Monitoring – An Int. J.*, Sage Pub., **1**(1), July 41-61.
- Giurgiutiu, V. (2003), "Embedded ultrasonics NDE with piezoelectric wafer active sensors", *J. Instrumentation, Measurement, Metrologie*, Lavoisier Pub., Paris, France, RS series 12M, **3**(3-4), 149-180.
- Ihn, J.-B. and Chang, F.-K. (2002), "Multi-crack growth monitoring at riveted lap joints using piezoelectric patches", *Proceedings of SPIE's 7th Annual International Symposium on NDE for Health Monitoring and Diagnostics*, 17-21 March 2002, San Diego, CA, **4702**, 29-40.
- Ihn, J.-B. (2003), "Built-in diagnostics for monitoring fatigue crack growth in aircraft structures", PhD Dissertation, Stanford University, Department of Aeronautics and Astronautics.
- Lin, X. and Yuan, F. G. (2001a) "Diagnostic Lamb waves in an integrated piezoelectric sensor/actuator plate: analytical and experimental studies", *Smart Mater. Struct.*, **10**, 907-913.
- Lin, X. and Yuan, F. G. (2001b) "Damage detection of a plate using migration technique", *J. Intelligent Mater. Sys. Struct.*, **12**(7), July 2001.
- Lin, X. and Yuan, F. G. (2001c), "Detection of multiple damage by prestack reverse-time migration", *AIAA J.*, **39**(11), Nov. 2206-2215.
- Liu, T., Veidt, M. and Kitipornchai, S. (2003), "Modeling the input-output behavior of piezoelectric structural health monitoring systems for composites plates", *Smart Mater. Struct.*, **12**, 836-844.
- Park, G., Sohn, H., Farrar, C. R. and Inman, D. J. (2003), "Overview of piezoelectric impedance-based health monitoring and path forward", *The Shock Vib. Digest*, **35**, 451-463.